International Journal of Microwave and Wireless Technologies

cambridge.org/mrf

A compact CPW-fed monopole antenna for multi-band application

YunYan Zhou[1,2], NianShun Zhao[1], RenXia Ning[3] and Jie Bao[1,2]

[1]College of Mechanical and Electrical Engineering, Huangshan University, 245041 Huangshan, Anhui Province, China; [2]Advance Package Technology Research Center of Huangshan University, 245041 Huangshan, Anhui Province, China and [3]College of Information Engineering, Huangshan University, 245041 Huangshan, Anhui Province, China

Research Paper

Cite this article: Zhou YY, Zhao NS, Ning RX, Bao J (2022). A compact CPW-fed monopole antenna for multi-band application. *International Journal of Microwave and Wireless Technologies* **14**, 995–1001. https://doi.org/10.1017/S1759078721001318

Received: 27 February 2021
Revised: 9 August 2021
Accepted: 14 August 2021
First published online: 17 September 2021

Keywords:
Multi-band; monopole antenna; CPW-fed; low frequency

Author for correspondence:
YunYan Zhou,
E-mail: yanwork@hsu.edu.cn

Abstract

A compact coplanar waveguide-fed monopole antenna is presented in this paper. The proposed antenna is composed of three monopole branches. In order to achieve the miniaturization, the longest branch was bent. The antenna is printed on an FR4 dielectric substrate, having a compact size of $0.144\lambda_0 \times 0.105\lambda_0 \times 0.003\lambda_0$ at its lowest resonant frequency of 900 MHz. The multiband antenna covers five frequency bands: 820–990 MHz, 1.87–2.08 GHz, 2.37–2.93 GHz, 3.98–4.27 GHz, and 5.47–8.9 GHz, which covers the entire radio frequency identification bands (860–960 MHz, 2.4–2.48 GHz, and 5.725–5.875 GHz), Global System for Mobile Communications (GSM) bands (890–960 MHz and 1.850–1.990 GHz), WLAN bands (2.4–2.484 GHz and 5.725–5.825 GHz), WiMAX band (2.5–2.69 GHz), X-band satellite communication systems (7.25–7.75 GHz and 7.9–8.4 GHz), and sub 6 GHz in 5G mobile communication system (3.3–4.2 GHz and 4.4–5.0 GHz). Also, the antenna has good radiation characteristics in the operating band, which is nearly omnidirectional. Both the simulated and experimental results are presented and compared and a good agreement is established. The proposed antenna operates in five frequency bands with high gain and good radiation characteristics, which make it a suitable candidate in terminal devices with multiple communication standards.

Introduction

With the development of wireless communication technology, more and more spectrum is being developed and utilized, and many terminal devices need to work in multiple frequency bands. The multi-band technology of the antenna allows a single antenna to realize multiple working frequency bands in multiple communication standards, which is gaining increasing attention. Researchers have proposed a series of methods, such as gap loading technology [1–8], multi-branch technology [9–15], reconfigurable technology [16, 17], loading a soft magnetic ferrite film [18], and so on.

A tri-band E-shaped printed antenna with C-shaped slots was presented by Kim Ho Yeap [1], which operated at a tri-band of 1.51/2.46/6.11 GHz. A coplanar waveguide (CPW)-fed compact tri-band antenna composed of three monopole radiators is proposed by Liu in [9]. The antenna works at three bands 2.36–2.82, 3.28–3.88, and 4.50–6.53 GHz for WLAN/WiMAX application. Ullah proposed an antenna that works at six frequencies: 2.10, 2.40, 3.35, 3.50, 5.28, and 5.97 GHz for Wi-Fi, 3G advanced, WiMAX, and WLAN wireless applications; the antenna uses reconfigurable technology, operates in four different frequency modes by the state of the two lumped element switches [16]. However, as the size of the antenna increases with decreasing frequency, the present multi-band antenna technology is mainly concentrated above 1 GHz, and the research on multi-band antenna below 1 GHz is relatively few. On the other hand, low-frequency communication has the advantages of long coverage distance, and many communication frequencies are lower than 1 GHz, such as GSM 850/900, radio frequency identification (RFID), etc.

A multiband planar antenna was reported in [13], which covers four frequency bands (−6 dB impedance): 696–970 MHz, 683–2700 MHz, 3070–3755 MHz, and 4590–7604 MHz. The size of the antenna is 15 mm × 65 mm, and the dimension of ground plane is 110 mm × 65 mm. In [18], by loading a soft magnetic ferrite film on the strong radiation area, the frequencies (−6 dB impedance) shifted to cover the range of 692–1191 MHz and 1698–3020 MHz. The antenna area occupies a size of 11 mm × 30 mm on the left corner above the system circuit board which has a standard dimension of 115 mm × 60 mm. These planar antennas have a low profile, but they need a large ground plane.

A planar monopole antenna with added L- and U-shaped monopoles was presented in [12] to provide four operating bands: 858–931 MHz, 1.571–2.845 GHz, 3.42–4.42 GHz, and 5.26–6.32 GHz. In [15], a monopole reader antenna for RFID portable devices was developed to

© The Author(s), 2021. Published by Cambridge University Press in association with the European Microwave Association

CAMBRIDGE UNIVERSITY PRESS

cover three frequency bands: 902–928 MHz, 2.4–2.48 GHz, and 5.725–5.875 GHz. However, the size of the antenna is too large for the miniaturization of the terminal devices.

In [8], an antenna of size 30 mm × 30 mm for RFID applications was reported, operating at 0.915–0.925, 2.425–2.455, and 5.45–6.16 GHz. However, the gain at the low resonant frequency 0.92 GHz was only −12.1 dBi.

Moreover, the available designs have a small number of frequency bands, narrow frequency coverage, which cannot meet the application requirements of multiple communication standards [19, 20].

The main factor that differentiates our study from the summarization study is a compact multiband antenna without large ground plane, which covers the lowest frequency band 820–990 MHz, and the highest band 5.47–8.9 GHz. With three branches, the antenna resonate at five frequencies (−10 dB impedance) 0.9/2.0/2.7/4.15/5.8 GHz, the simulated gain at the five frequencies is −3.30, 0.82, 1.08, 3.42, and 3.00 dBi, respectively, which can meet RFID (0.92/2.45/5.8 GHz), GSM900 (0.9 GHz), GSM1900 (1.9 GHz), WLAN (2.4/5.8 GHz), WiMAX (2.5 GHz), sub 6 GHz in 5G mobile communication system, satellite communication, and other application requirements.

Antenna description

Antenna structure

The traditional monopole antenna is formed by removing one arm of the dipole antenna according to the mirror principle through an infinite ground plane. The planar monopole and the ground plane of the proposed antenna are printed on the same side of the dielectric substrate. Impedance matching is achieved by adjusting the ground area and the gap size between the monopole and the ground.

The length of monopole antenna is about a quarter wavelength, and the wavelength λ of electromagnetic wave in free space can be calculated by using equation (1). However, due to the use of a dielectric substrate, part of the electromagnetic wave propagates in free space, while the other part propagates in the dielectric substrate. The wavelength λ_e in the dielectric substrate is determined by using equation (2). Therefore, the wavelength corresponding to the length of monopole should be between λ and λ_e:

$$\lambda = \frac{c}{f} \tag{1}$$

$$\lambda_e = \frac{c}{f\sqrt{\varepsilon_r}} \tag{2}$$

where c represents the propagation velocity, f represents the frequency of the electromagnetic wave, and ε_r represents the dielectric constant of the dielectric substrate.

Configuration of the proposed antenna is shown in Fig. 1. The antenna was designed on a low cost FR4 substrate, with a dielectric constant of 4.4, loss tangent angle of 0.02, and thickness of 1 mm. The antenna is fed by a CPW. In order to achieve multiband coverage, the monopole adopts three branches with different lengths. Because the wavelength of low frequency 900 MHz is very long, the longest branch was bent to achieve the miniaturization of the antenna. The space occupied by the left and right branches is different, the ground plane of the short branch is cut accordingly, and then the feeding position is not in the central position of the antenna.

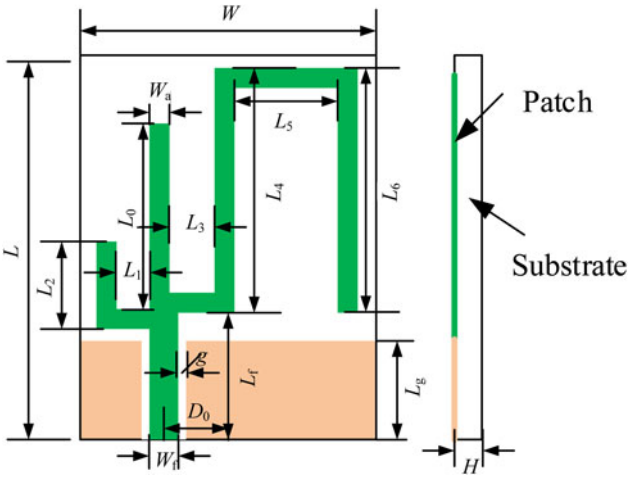


Fig. 1. Geometry of the proposed antenna.

Table 1. Lengths of the three branches

	5.8 GHz		2.0 GHz	900 MHz			
Parameters	L_1	L_2	L_0	L_3	L_4	L_5	L_6
Calculated (mm)	3	7	25	8	32	10	25
Simulated (mm)	3	9	26	6	31	13	31

According to the quarter wavelength of formulas (1) and (2), the initial length and the final optimized simulation length of each branch are shown in Table 1. The shortest branch is 10 mm for 5.8 GHz, the longest branch is 75 mm for 900 MHz, and the middle length branch is 25 mm for 2 GHz.

Principle of operation

In order to explain the principle of the antenna, several key parameters are studied as shown in Fig. 2. In Fig. 2(a), it can be seen that the length L_2 of the shortest branch mainly affects the high-frequency bands, and has no effect on the low frequency 0.9/2.0 GHz. As L_2 increases, the resonant frequency moves to low frequency. Figure 2(b) depicts the effect of the length L_0 of the middle branch. L_0 mainly affects 2.0/2.7/5.8 GHz, has no effect on low frequency 0.9 GHz, and has little effect on 4.15 GHz. The impact of the length L_6 of the longest branch on the antenna is shown in Fig. 2(c). The low-frequency resonant frequency decreases with the increase of L_6, but L_6 has no effect on the high frequency of 5.8 GHz. Figure 2(d) illustrates that the length of L_f of the feed microstrip line affects the impedance matching of all resonant frequency points. Meanwhile, as the L_f increases, the resonant frequency decreases in the high band. However, it has almost no effect on the 0.9 GHz resonant frequency, because the length of the branch in this frequency is much longer than L_f, and the change of L_f has little effect on the total length, so it does not affect the resonant frequency.

The surface current distribution of the antenna at five different resonant frequencies is shown in Fig. 3. In Fig. 3(a), the current mainly flows at the longest branch, it indicates that the low-

https://doi.org/10.1017/S1759078721001318 Published online by Cambridge University Press

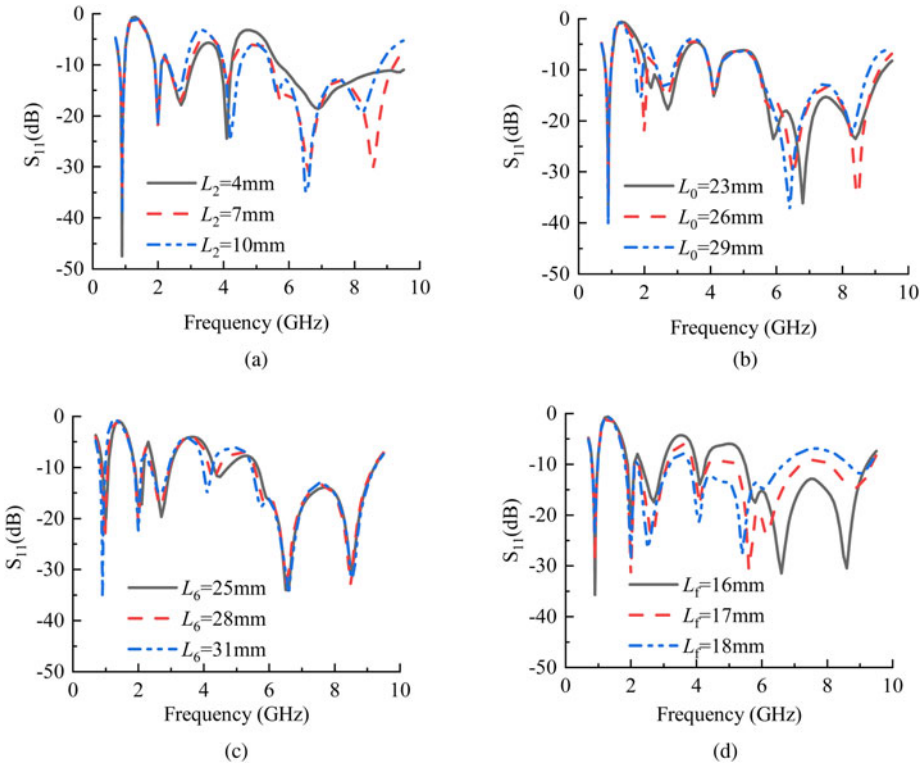


Fig. 2. Simulated S_{11} for different lengths of (a) L_2, (b) L_0, (c) L_6, and (d) L_f.

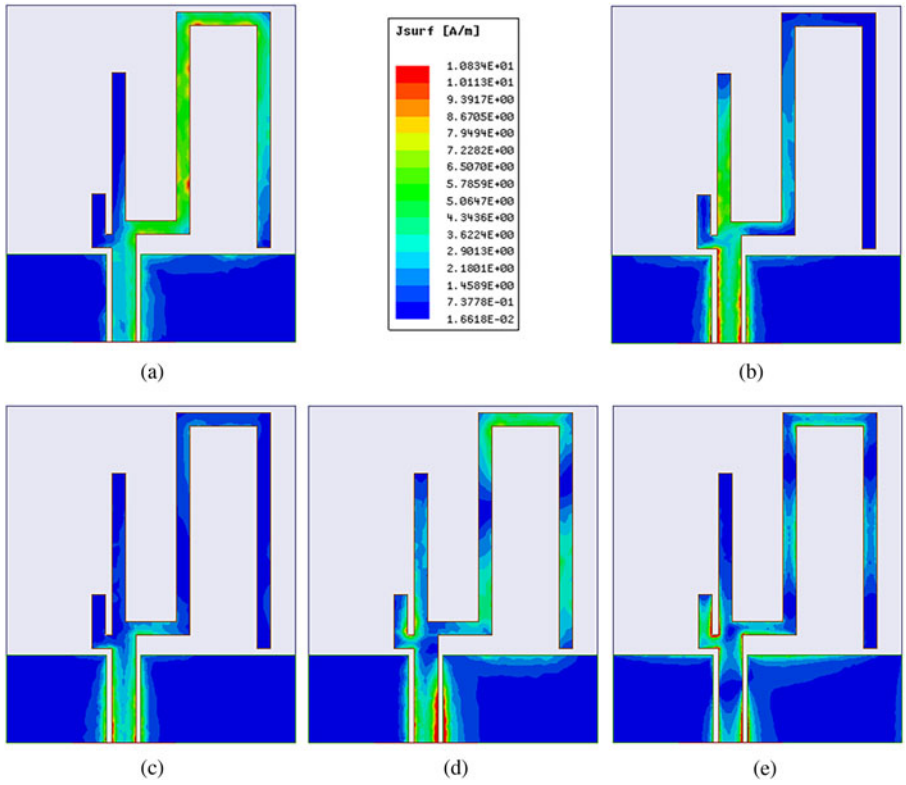


Fig. 3. Surface current distributions of at different frequencies: (a) 0.9 GHz, (b) 2.0 GHz, (c) 2.7 GHz, (d) 4.15 GHz, and (e) 5.8 GHz.

https://doi.org/10.1017/S1759078721001318 Published online by Cambridge University Press

Table 2. Dimensions for the proposed antenna

Parameters	L	W	H	L_g	L_f	W_f	g	D_0
Value (mm)	48	35	1	13	16	2.5	0.8	9
Parameters	W_a	L_0	L_1	L_2	L_3	L_4	L_5	L_6
Value (mm)	2	26	3	9	6	31	13	31

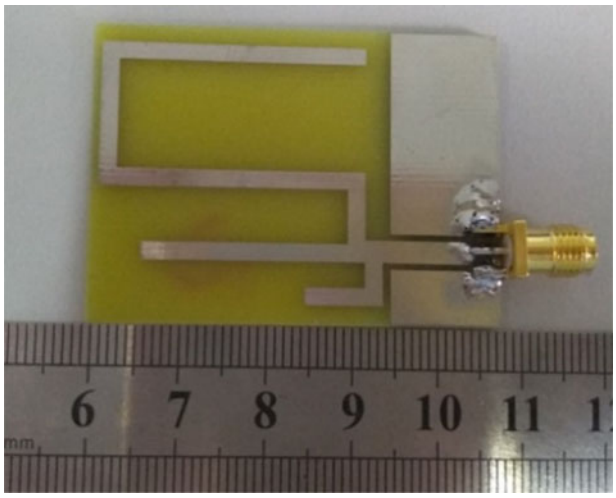


Fig. 4. Prototype of the proposed antenna.

frequency band at 0.9 GHz is determined by the longest branch. The current at 2.0 GHz spreads at the middle branch with middle length as shown in Fig. 3(b). At the resonant frequency of 2.7 GHz, the strong current flows at the microstrip line and the left short branch. In Fig. 3(d), we can see that the strong current distributes at the longest branches, but two obvious current zero points can be seen, indicating that the resonance point is in the form of high mode. The highest frequency 5.8 GHz current spreads at the shortest branch. The current distributions are consistent with the previous parameter analysis results.

Results and discussion

Through detailed simulation and optimization, the dimensions of the antenna are shown in Table 2. The prototype is fabricated and displayed in Fig. 4. Measured results of return loss and radiation patterns were obtained by a network analyzer and a chamber antenna measurement system, and Fig. 5 shows the actual environment of far-field radiation characteristics measurements. Experimental results show that the proposed antenna with a compact size of 48 mm × 35 mm × 1 mm has good impedance matching and nearly omnidirectional radiation patterns at five resonant bands.

Figure 6 depicts simulated and measured return loss of the proposed antenna. There is reasonably good agreement between the measured and the simulated results. It can be seen that the antenna has −10 dB impedance band widths of 170 MHz (0.820–0.990 GHz), 210 MHz (1.87–2.08 GHz), 560 MHz (2.37–2.93 GHz), 290 MHz (3.98–4.27 GHz), and 3.43 GHz (5.47–8.9 GHz). The first band is essentially useful for the RFID (860–960 MHz) and GSM900 (890–915 MHz and 935–960 MHz). The second band finds wide applications in the GSM. The third band serves the RFID (2.4–2.483 GHz), WLAN (2.4–2.484 GHz), and WiMAX (2.5–2.69 GHz). The fourth frequency band can be used for 5G communications. And the fifth band is essentially useful for RFID and WLAN (5.725–5.875 GHz), the WiFi 6 band form the IEEE 802.11ax (5.925–7.125 GHz), and the unlicensed frequency bands are commonly used for satellite communications, and may soon be opened for mobile services.

The simulation peak gain and radiation efficiency of the antenna are depicted in Fig. 7. The gains of the resonant frequencies we interest at 0.9/2.0/2.7/4.15/5.8 GHz are −3.30/0.82/1.08/3.42/3.00 dBi respectively. The highest peak gain is 5.1 dBi, the mid-to-high-frequency band does not change much. But, the gain of the low-frequency band is significantly reduced due to the reduction of the antenna size, which will shorten the radiation distance of the antenna. The minimum gain is −4 dBi in 0.820–0.990 GHz bandwidth. The radiation efficiency of the antenna in the operated bands is more than 88%, and reached a maximum of 96%, while a huge decrease in antenna efficiency is noticed at 1.3 GHz. This sudden decrease in efficiency shows that the antenna cannot operate in this band.

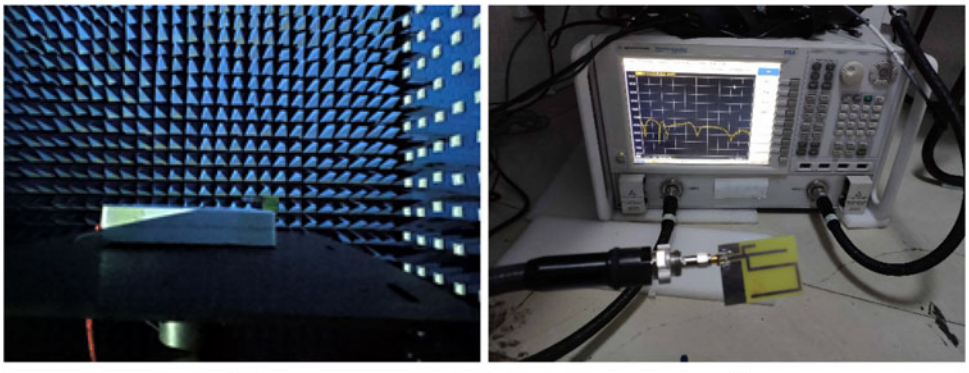


Fig. 5. Prototype of the measurement environment: (a) far-field radiation characteristics and (b) return loss.

https://doi.org/10.1017/S1759078721001318 Published online by Cambridge University Press

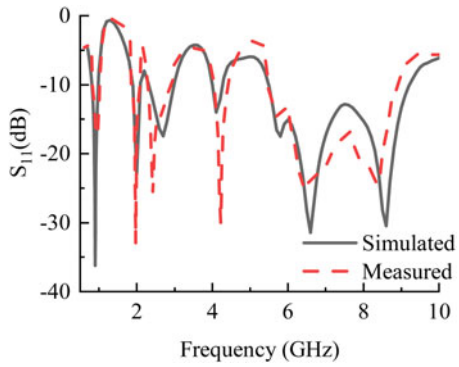


Fig. 6. Simulated and measured return loss S_{11} of the proposed antenna.

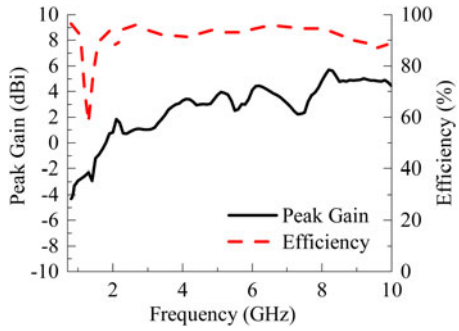


Fig. 7. Simulated peak gain and efficiency of the antenna.

The simulated and measured radiation patterns in the *xz* plane and *yz* plane at five resonant frequencies are shown in Fig. 8. In the *yz* plane at the five resonant frequencies the radiation patterns are approximately circular, indicating that the antenna has good omni-directionality.

In Table 3, the performance of the proposed multiband antenna is compared with the antennas reported in the literature, which can cover the frequency band below 1 GHz. The size comparisons are performed based on the air wavelength λ_0 at the lowest resonant frequency. The bandwidths are −10 dB impedance bandwidth in [8, 12, 14, 15], while the bandwidths are −6 dB impedance bandwidth in [13, 18]. The −10 dB impedance bandwidth in [13, 18] is smaller than the given value in the table. The proposed antenna has compact size with simple structure, without large ground plane. At the lowest resonant frequency 900 MHz, the size of the proposed antenna is much smaller than a quarter wavelength from equations (1) and (2). Although the dimension of the proposed antenna is a little larger than that in [8], the antenna gain at 900 MHz is −3.30 dBi, which is much higher than −12 dBi in [8]. And the proposed antenna has the widest impedance band and the maximum number of frequency bands, which covers the lower band 0.82–0.99 GHz and the higher band 5.47–8.9 GHz.

Conclusion

A compact CPW-fed monopole antenna with three branches is designed, fabricated, and tested. According to the measured

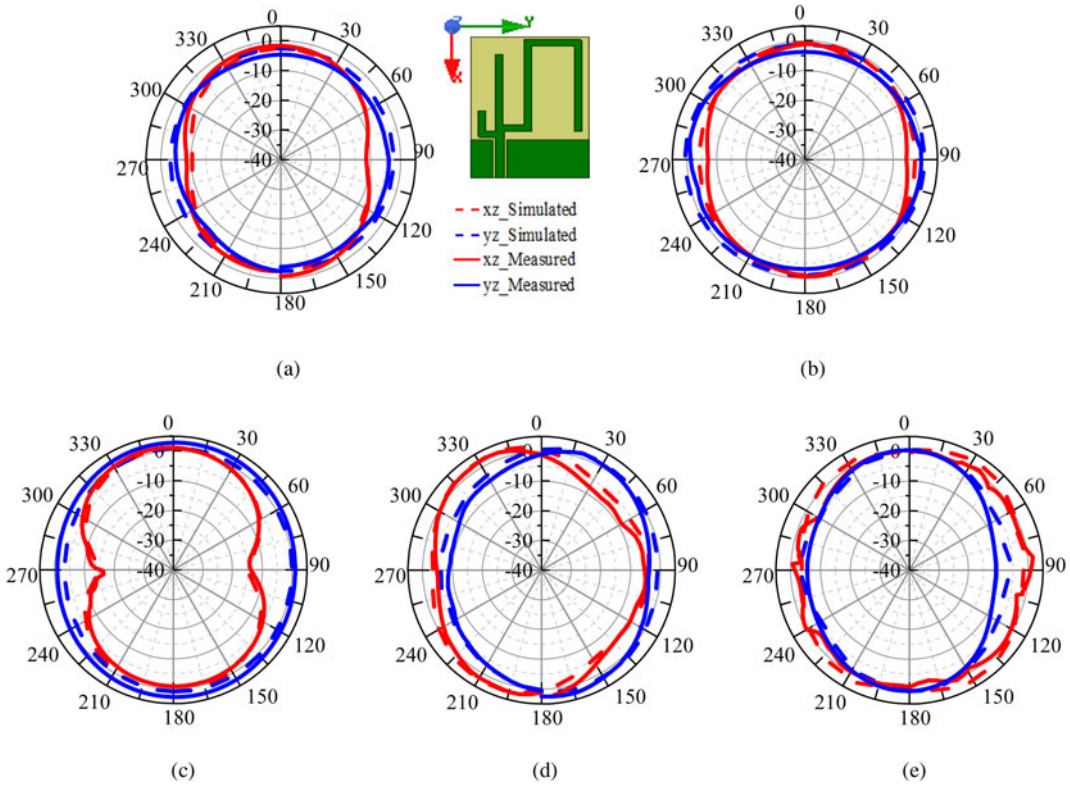


Fig. 8. Measured and simulated radiation patterns of the proposed antenna at *xz* plane and *yz* plane: (a) 0.9 GHz, (b) 2.0 GHz, (c) 2.7 GHz, (d) 4.15 GHz, and (e) 5.8 GHz.

https://doi.org/10.1017/S1759078721001318 Published online by Cambridge University Press

Table 3. Comparison of the proposed antenna with existed literatures

Ref.	Size	Bandwidth (GHz)	Gain (dBi)
[8]	$0.092\lambda_0 \times 0.092\lambda_0 \times 0.005\lambda_0$	0.915–0.925	−12.1 (0.92 GHz)
		2.425–2.455	−1.7 (2.45 GHz)
		5.45–6.16	5.2 (5.8 GHz)
[12]	$0.276\lambda_0 \times 0.144\lambda_0 \times 0.0048\lambda_0$	0.858–0.941	1.83 (0.901 GHz)
		1.57–2.845	2.98 (2.4 GHz)
		3.42–4.429	2.33 (3.73 GHz)
		5.26–6.32	2.91 (5.9 GHz)
[13]	$0.174\lambda_0 \times 0.04\lambda_0 \times 0.0013\lambda_0$ Ground: $0.17\lambda_0 \times 0.29\lambda_0$	0.696–0.97	2.5 (0.800 GHz)
		1.683–2.7	3.2 (2 GHz)
		3.07–3.755	4.5 (3.5 GHz)
		4.59–7.604	5.4 (5.5 GHz)
[15]	$0.35\lambda_0 \times 0.07\lambda_0 \times 0.0049\lambda_0$	0.883–1.560	2.2 (0.915 GHz)
		2.31–2.89	5.5 (2.4 GHz)
		5.645–5.9	7.5 (5.8 GHz)
[18]	$0.026\lambda_0 \times 0.07\lambda_0 \times 0.002\lambda_0$ Ground: $0.268\lambda_0 \times 0.14\lambda_0$	0.692–1.191	−5.0 (0.698 GHz)
		1.698–3.020	5.9 (2.35 GHz)
Proposed	$0.144\lambda_0 \times 0.105\lambda_0 \times 0.003\lambda_0$	0.82–0.99	−3.30 (0.90 GHz)
		1.87–2.08	0.82 (2.0 GHz)
		2.37–2.93	1.08 (2.7 GHz)
		3.98–4.27	3.42 (4.15 GHz)
		5.47–8.9	3.00 (5.8 GHz)

results, the −10 dB matching bandwidth is 170 MHz (820–990 MHz), 210 MHz (1.87–2.08 GHz), 560 MHz (2.37–2.93 GHz), 290 MHz (3.98–4.27 GHz), and 3.43 GHz (5.47–8.9 GHz). The radiation pattern in the *yz* plane of the antenna is nearly omnidirectional. The minimum antenna gain is −3.30 dBi at the lowest resonant frequency 900 MHz. The antenna may be applied to terminal devices of wireless communication system with multiple communication standards.

Acknowledgement. This study was supported by the Natural Science Research Project of Education Department of Anhui Province (KJHS2020B14, KJ2020A0684, and KJHS2019B01), and the Science & Technology Project of Huangshan City (2020KG-04).

References

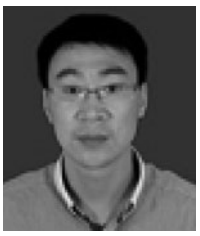
1. **Yeap KH, Yeo WL, Lai KC and Xo Z** (2020) A compact E-shaped antenna with C-shaped slots and a back-patch for multiband applications. *Journal of Electrical Engineering* **71**, 49–54.
2. **Kumar R, Naidu VP and Kamble V** (2015) Simulation, design of compact multi-band microstrip slot antennas for WiMAX/WLAN and UWB applications. *Wireless Personal Communications* **80**, 1175–1192.
3. **Kumar A, Deegwal JK and Sharma MM** (2019) Miniaturized multistubs loaded rectangular monopole antenna for multiband applications based on theory of characteristics modes. *Progress in Electromagnetics Research C* **92**, 131–137.
4. **Jalali AR, Ahamdi-Shokouh J and Emadian SR** (2016) Compact multiband monopole antenna for UMTS, WiMAX, and WLAN applications. *Microwave and Optical Technology Letters* **58**, 844–847.
5. **Moosazadeh M and Kharkovsky S** (2014) Compact and small planar monopole antenna with symmetrical L- and U-shaped slots for WLAN/WiMAX applications. *IEEE Antennas and Wireless Propagation Letters* **13**, 388–391.
6. **Dewan R, Rahim M, Himdi M, Hamid MR, Majid HA and Jalil ME** (2017) Multiband frequency-reconfigurable antenna using metamaterial structure of electromagnetic band gap. *Applied Physics A* **123**, 16–18.
7. **Khan Z, Memon MH and Rahman SU** (2020) A single-fed multiband antenna for WLAN and 5G applications. *Sensors* **20**, 1–13.
8. **Li HH, Mou XQ, Ji Z, Yu H, Li Y and Jiang L** (2011) Miniature RFID tri-band CPW-fed antenna optimised using ISPO algorithm. *Electronics Letters* **47**, 161–162.
9. **Liu T, Sun YF and Li J** (2019) CPW-fed compact multiband monopole antenna for WLAN/WiMAX/X-band application. *Progress in Electromagnetics Research* **87**, 105–113.
10. **Wu L, Huang J and Yuan N** (2016) Compact multiband monopole antenna for GPS/WLAN/WiMAX application. IEEE International Conference on Microwave and Millimeter Wave Technology (ICMMT), Beijing.
11. **Kumar PV and Harish AR** (2018) A compact CPW-fed tapered monopole triple-band antenna for WLAN/WiMAX application. *Microwave & Optical Technology Letters* **60**, 2298–2303.
12. **Yousuf S and Tlili B** (2012) Multiband planar branched monopole antenna for GSM/GPS/WLAN/WiMAX applications. IEEE Antennas and Propagation Society International Symposium, Chicago.
13. **Cui Y, Yang L, Liu B and Li R** (2016) Multiband planar antenna for LTE/GSM/UMTS and WLAN/WiMAX handsets. *Microwaves, Antennas and Propagation* **10**, 502–506.
14. **Mandal D and Pattnaik SS** (2019) Wide CPW-fed multiband wearable monopole antenna with extended grounds for GSM/WLAN/WiMAX applications. *International Journal of Antennas & Propagation* **10**, 1–14.
15. **Wang B and Wang W** (2017) A miniature tri-band RFID reader antenna with high gain for portable devices. *International Journal of Microwave and Wireless Technologies* **9**, 1163–1167.

https://doi.org/10.1017/S1759078721001318 Published online by Cambridge University Press

16. **Ullah S, Ahmad S, Khan BA and Flint JA** (2018) A multi-band switchable antenna for Wi-Fi, 3G advanced, WiMAX, and WLAN wireless applications. *International Journal of Microwave and Wireless Technologies* **10**, 991–997.
17. **Mansoul A and Seddiki ML** (2018) Multiband reconfigurable bowtie slot antenna using switchable slot extensions for WiFi, WiMAX, and WLAN applications. *Microwave and Optical Technology Letters* **60**, 413–418.
18. **Wu T, Yu G, Pang J, Wang C and Zhou HM** (2020) The low-frequency improvement with loading soft magnetic ferrite films for multiband antenna applications. *International Journal of Applied Electromagnetics and Mechanics* **6**, 1–10.
19. **Wang D and Chan CH** (2016) Multiband antenna for WiFi and WiGig communications. *IEEE Antennas and Wireless Propagation Letters* **15**, 309–312.
20. **Singh G, Kanaujia BK, Pandey VK, Gangwar D and Kumar S** (2019) Design of compact dual-band patch antenna loaded with D-shaped complementary split ring resonator. *Journal of Electromagnetic Wave* **16**, 2096–2111.



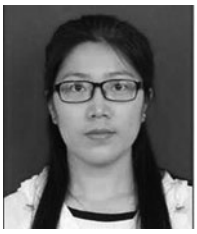
YunYan Zhou received her M.S. degree in circuits and systems from Anhui University, Anhui Province, China, in 2009. She is a lecturer in the College of Mechanical and Electrical Engineering, Huangshan University, Anhui Province, China. Her current research interest is in planar antenna design.



NianShun Zhao received his Ph.D. in 2018 from Northwest Polytechnical University, Shaanxi Province, China. He is an associate professor in the College of Mechanical and Electrical Engineering, Huangshan University. He has authored more than 30 research articles. He is active in the study of functional ceramic materials.



RenXia Ning received her M.S. degree in circuits and systems from Anhui University, Anhui Province, China. She is an associate professor in the College of Information Engineering of Huangshan University, Anhui Province, China. She has authored more than 20 research articles. Her current research interest is electromagnetic properties and applications of graphene.



Jie Bao received her Ph.D. in 2017 from Shanghai University, Shanghai, China. She is a professor in the College of Mechanical and Electrical Engineering, Huangshan University, China. She has authored more than 30 research articles. Her current research interest is semiconductor packaging technology.

https://doi.org/10.1017/S1759078721001318 Published online by Cambridge University Press